Cancer-associated fibroblasts in renal cell carcinoma: implication in prognosis and resistance to anti-angiogenic therapy

Damien Ambrosetti, Michael Coutts, Charlotte Paoli, Matthieu Durand, Delphine Borchiellini, Christopher Montemagno, Olivia Rastoin, Arnaud Borderie, Renaud Grepin, Nathalie Rioux-Leclercq, et al.

▶ **To cite this version:**

Damien Ambrosetti, Michael Coutts, Charlotte Paoli, Matthieu Durand, Delphine Borchiellini, et al.. Cancer-associated fibroblasts in renal cell carcinoma: implication in prognosis and resistance to anti-angiogenic therapy. BJU International, 2022, 129 (1), pp.80-92. 10.1111/bju.15506 . hal-03476907

HAL Id: hal-03476907
https://hal.science/hal-03476907

Submitted on 12 Jan 2022

HAL is a multi-disciplinary open access archive for the deposit and dissemination of scientific research documents, whether they are published or not. The documents may come from teaching and research institutions in France or abroad, or from public or private research centers.

L'archive ouverte pluridisciplinaire **HAL**, est destinée au dépôt et à la diffusion de documents scientifiques de niveau recherche, publiés ou non, émanant des établissements d'enseignement et de recherche français ou étrangers, des laboratoires publics ou privés.

Distributed under a Creative Commons Attribution - NonCommercial 4.0 International License

Cancer associated fibroblasts in Renal Cell Carcinoma: implication in prognosis and resistance to antiangiogenic therapy

Damien Ambrosetti[1,2$], Michael Coutts[3], Charlotte Paoli[1], Matthieu Durand[4], Delphine Borchiellini[5], Christopher Montemagno[2,6,7], Olivia Rastoin[2,7], Arnaud Borderie[1], Renaud Grepin[6,7], Nathalie Rioux-Leclercq[8], Jean-Christophe Bernhard[9,10], Gilles Pagès[2,6,7], Maeva Dufies[6,7$]

1. Department of Pathology, Université Côte d'Azur, CHU Nice, Nice, France.
2. University Côte d'Azur, Institute for Research on Cancer and Aging of Nice (IRCAN), CNRS UMR 7284; INSERM U1081, Centre Antoine Lacassagne, 06189 Nice, France
3. Department of Pathology, Maidstone General Hospital, Maidstone.
4. Department of Urology, Université Côte d'Azur, CHU Nice, Nice, France
5. Department of Oncology, Centre Antoine Lacassagne, Nice, France.
6. Department of Biomedical, Centre Scientifique de Monaco, Principality of Monaco.
7. LIA ROPSE, Laboratoire International Associé Université Côte d'Azur - Centre Scientifique de Monaco, Principality of Monaco
8. Department of Pathology, University Hospital, Rennes, France
9. Department of Urology, University Hospital, Bordeaux, France
10. French Research Network on Kidney Cancer UroCCR , Bordeaux, France

$ Corresponding authors: Damien Ambrosetti (ambrosetti.d@chu-nice.fr) and Maeva Dufies (maeva.dufies@gmail.com)

Accepted Article

This article has been accepted for publication and undergone full peer review but has not been through the copyediting, typesetting, pagination and proofreading process, which may lead to differences between this version and the Version of Record. Please cite this article as doi: 10.1111/BJU.15506

Accepted Article

DR. DAMIEN AMBROSETTI (Orcid ID : 0000-0001-8665-0546)
DR. MATTHIEU DURAND (Orcid ID : 0000-0001-6335-8067)

Article type : Original Article

ABSTRACT

OBJECTIVES:

To investigate the role of cancer-associated fibroblasts (CAFs) in clear cell renal cell carcinoma (ccRCC) with respect to tumor aggressiveness, metastasis development and resistance to antiangiogenic therapy (VEGFR-tyrosine kinase inhibitors, VEGFR-TKI).

METHODS:

Our study involved tissue samples from three distinct and independent cohorts of patients with ccRCC. The presence of CAFs and tumor lymphangiogenesis was investigated respectively by transcriptional signatures and then correlated with tumor development and prognosis. The effect of these CAFs on tumor cell migration and VEGFR-TKI resistance was analyzed on co-cultures of ccRCC cells with CAFs.

RESULTS:

Results from our cohorts and from *in silico* investigations showed that VEGFR-TKI significantly increase the number of CAFs in tumors. In the same populations of ccRCC patients, the proportion of intra-tumoral CAFs correlated to shorter disease-free and overall survival. The presence of CAFs was also correlated with lymphangiogenesis and lymph node metastasis. CAFs increased the migration and decrease the VEGFR-TKI-dependent cytotoxic effect of tumor cells.

CONCLUSIONS:

Accepted Article

Our results showed that VEGFR-TKI promote the development of CAFs, and CAFs favor tumor aggressiveness, metastatic dissemination and resistance to treatment in ccRCC. CAFs could represent a new therapeutic target to fight resistance to treatment of ccRCC. Targeting CAF and immunotherapies combination are emerging as efficient treatments in many types of solid tumors. Our results highlight their relevance in ccRCCs.

KEY WORDS: clear cell renal cell carcinoma (ccRCC), cancer associated fibroblasts (CAF), FAP, prognostic marker, antiangiogenic treatment, resistance.

INTRODUCTION

Renal cancer is the 6th most common cancer in men and 9th in women. It is the third urologic cancer in terms of incidence and mortality (1). Recently, the management of renal cancer and the understanding of its biology have been the subject of great progresses. Thus, different histological subtypes have been identified, characterized by distinct genetic and molecular alterations, corresponding to different pathways of oncogenesis, inhibited by targeted therapies.

The World Health Organization classification which was revised in 2016 distinguishes 13 subtypes of Renal Cell Carcinoma (RCC). Of these, clear cell renal cell carcinoma (ccRCC) is the most common histologic subtype (70-75% of all kidney cancers) (2). More than 90% of ccRCC exhibits a loss of function of the von Hippel-Lindau tumor suppressor gene (VHL), leading to stabilization of hypoxia-inducible factors HIF and upregulation of genes responsible for angiogenesis (VEGF). Almost a third of these patients present with unresectable or metastatic tumors for whom surgery is not an appropriate management option. Anti-VEGFR tyrosine kinase inhibitors (VEGFR-TKI, such as sunitinib and axitinib) and immunotherapies (such as nivolumab and ipilimumab) have successively led to a radical change in patient management and represent significant therapeutic options in the treatment of advanced ccRCC (3). To further enhance the benefits of these treatments, different combinations, and sequences of TKI and immunotherapies are being investigated in clinical trials (4). Patients who relapse on these therapies are left with very few options.

Accepted Article

It is important to identify the mechanisms of resistance, to assess their importance and to propose rational therapeutic approaches to obtain additional clinical benefits (5). Neoangiogenesis, the development of a tumor vasculature, is key to provide the nutritional needs of cancer cells and for tumor growth beyond a few millimeters.

Tumor stroma is made up of diverse populations of cells of mesenchymal origin included in the extracellular matrix. These cells are fibroblasts, endothelial, inflammatory, and mesenchymal stem cells. The tumor microenvironment is qualitatively and quantitatively variable depending on the organ in which the tumor develops and depending on the type of tumor. The stromal reaction is reduced in ccRCC and the microenvironment is often reduced to the capillary network activated by the VHL-HIF-VEGF pathway (6). This tumor stroma will change over time and during the process of tumor development, according to the interactions that can occur between tumor cells and stromal cells. Treatments can also modify the tumor's stroma.

Among the stromal cells appearing during these mechanisms, cancer-associated fibroblasts (CAFs) are of particular importance. TGFβ and PDGF induce differentiation of tumor fibroblasts into CAFs (7). CAFs produce numerous pro-tumoral cytokines (including IL6, IL8, IL10, TNFα, TGFβ) and generate a collagen matrix which hinders the action of T lymphocytes within the tumor. Indeed, CAFs play a very important role in tumor progression. They interact with cancer cells via a paracrine mechanism, promoting tumor development by creating an environment favorable to the tumor development and to the formation of metastases.

The histological changes induced by TKI have not been fully studied in ccRCC. In the present study, we therefore evaluated the tissue alterations induced by TKI. We hypothesized that these modifications are at the origin of the mechanisms leading to resistance to TKI. We specifically focused on CAFs.

MATERIALS AND METHODS

ccRCC patients

As defined by the 2016 World Health Organization criteria, diagnosis was based upon pathology and cytogenetic analysis. This retrospective study was approved by each

Accepted Article

institutional review board and was conducted in accordance with the Declaration of Helsinki.

Neoadjuvant cohort (Study cohort 1)

The neoadjuvant cohort included patients who underwent nephrectomy following neoadjuvant sunitinib (neoadjuvant cases, n=11) and patients who underwent nephrectomy without any prior treatment (control cases, n=11). Samples (tumor section) were obtained from Nice, Bordeaux (UroCCR, Clinical Trial: NCT03293563) and Monaco Hospitals. Neoadjuvant cases received oral sunitinib (50 mg per day) once daily for 4 weeks (on days 1 to 28), followed by 2 weeks without treatment. Patients were treated for at least two months before surgery (clinical characteristics in Table 1).

M0 cohort (Study cohort 2)

Tissue samples from 43 patients with non-metastatic ccRCC (M0) who had undergone surgery in the urology department of Rennes University Hospital were selected. The disease-free survival (DFS) and overall survival (OS) were calculated from patient subgroups with Fibroblast Associated Protein (FAP) mRNA levels that were less or greater than the third quartile value (clinical characteristics in Table 2).

Quantitative Real-Time PCR (qPCR) experiments

Renal tissues were collected from Study cohorts 1 and 2. Patients underwent radical or partial nephrectomy at the Department of Urology at University Hospital (Nice, Bordeaux, Monaco, Rennes). RNA from formalin-fixed, paraffin-embedded (FFPE) tissue sections was extracted and purified using RNeasy FFPE Kit (QIAGEN). 1 µg of total RNA was used for the reverse transcription, using the QuantiTect Reverse Transcription kit (QIAGEN), with a blend of oligo (dT) and random primers to prime first-strand synthesis. SYBR master mix plus (Eurogentec, Liege, Belgium) was used for qPCR. The mRNA level was normalized to 36B4 mRNA.

Accepted Article

Histochemistry, quantification of histologic parameters and immunohistochemical analyses

Formalin-fixed, paraffin-embedded (FFPE) sections were stained with HES and Masson Trichrome to evaluate deposition of interstitial collagen within the tumors. Stained slides were scanned using a Leica SCN400 Digital Slide Scanner (Leica Microsystems CMS GmbH, Wetzlar, Germany) at ×40 magnification. SlidePath software (Leica Microsystems) was used for image measurement. Capillary thickness was determined using Masson Trichrome stained slides. The first 20 capillaries, identified by morphology and size, were measured. Thickness was measured manually using a software built-in tool by two trained pathologists (DA, FV) blinded to the presurgical conditions. Same FFPE sections were used for immunohistochemical analyses. Immunolabeling and detection were performed using a Dako Autostainer AutoMate, according to the manufacturer's recommendations. The antibodies used were against FAP (ab53066, 1/100 dilution, high pH, Abcam, Toronto, ON), CD31 (JC70A, RTU, low pH, Dako), and smooth muscle actin (SMA, 1A4, RTU, low pH, Dako). The detection was performed using the Envision Flex Kit (Dako), with 3–3′ diaminobenzidine as a chromogen.

Gene expression microarray analysis (TCGA cohort, Study cohort 3)

Normalized RNA sequencing (RNA-Seq) data produced by The Cancer Genome Atlas (TCGA) were downloaded from cBiopotal (www.cbioportal.org, TCGA Provisional; RNA-Seq V2). Data were available for 503 of the 536 ccRCC tumor samples TCGA subjected to mRNA expression profiling. The clinical data were obtained through cBioPortal for Cancer Genomics and the 33 samples lacking classification were discarded. The non-metastatic group contained 424 patients and the metastatic group contained 79 patients. The results published here are in whole or in part based upon data generated by the TCGA Research Network ((7)). The progression free survival (PFS), DFS and OS were calculated from patient subgroups with FAP mRNA levels that were less or greater than the third quartile value. The Kaplan-Meier method was used to produce DFS, PFS and OS curves.

We also performed a score with the "CAF signature" including FAP, ACTA1 (SMA), COL1A1, TGFB1, LOXL2, PLOD3 mRNAs. When mRNA expression was high (third

quartile cut-off) a score of 1 was assigned. Scores of the six mRNA markers were pooled. Then patient groups were defined as follows; patients with a score of 0 (none marker overexpressed), patients with a score of 1 to 3 (1 to 3 overexpressed markers), and patients with a score between 4 and 6 (from 4 to 6 overexpressed markers).

Cell culture

786-0 (786) ccRCC cells were purchased from the American Tissue Culture Collection. Primary human fibroblasts were obtained from skin biopsies of a normal individual (FHN). FHN resistant cells (FHNR) were obtained by chronic exposure (2 months) to increasing concentrations of sunitinib, up to 10 µmol/L.

Cell viability (XTT)

Cells were incubated in a 96-well plate with different effectors for the times indicated in the figure legends. 50 µl of sodium 3′ - [1-phenylaminocarbonyl) -3,4- tetrazolium] - bis (4-methoxy-6-nitro) benzene sulfonic acid hydrate (XTT) reagent was added to each well. The assay is based on the cleavage of the yellow tetrazolium salt XTT to form an orange formazan dye by metabolically active cells. Absorbance of the formazan product, reflecting cell viability, was measured at 490 nm. Each assay was performed in quadruplicate.

Flow cytometry – sunitinib evaluation

Sunitinib is a lysosomotropic drug which is sequestered in lysosomes. Hence, the mean of autofluorescence of sunitinib inside the cells is quantifiable by cytometry (26).

The percentage of auto-fluorescent cells containing sunitinib was evaluated using the FITC (FL2) channel of a fluorescence-activated cell sorter apparatus (FACS-Calibur cytometer).

Migration assay

FHN/FHNR-dependent chemotaxis was monitored using modified Boyden chambers containing polycarbonate membranes (8-µm pores, Transwell; Corning, Sigma). 786

Accepted Article

Accepted Article

cells were seeded on the upper side of the filters and chambers were placed on 24-well plates containing FHN or FHNR at confluence and without serum. Cell migration was evaluated 24 hrs after seeding at 37°C in 5% CO2. Migrating cells on the lower membrane surface were fixed in 3% paraformaldehyde and stained with 0.1% crystal violet.

Statistical analyses

For patients

The Student's t-test was used to compare continuous variables and chi-square test, or Fisher's exact test (when the conditions for use of the $\chi 2$-test were not fulfilled), were used for categorical variables. DFS was defined as the time from surgery to the appearance of metastasis. OS was defined as the time between surgery and the date of death from any cause, censoring those alive at last follow-up. The Kaplan-Meier method was used to produce survival curves and analyses of censored data were performed using Cox models. All analyses were performed using R software, version 3.2.2 (Vienna, Austria, https://www.r-project.org/).

For in vitro analysis

All data are expressed as the mean ± the standard error (SEM). Statistical significance and p values were determined by the two-tailed Student's t-test. One-way ANOVA was used for statistical comparisons. Data were analyzed with Prism 5.0b (GraphPad Software) by one-way ANOVA with Bonferroni post hoc.

RESULTS

Sunitinib increases the thickness of vessel walls and the number of CAFs

To investigate the effect of sunitinib on micro-vascularization, we analyzed morphometric characteristics of capillaries. The vessel wall was statistically thicker in neoadjuvant cases (Fig. 1A, B) as compared to control cases (median thickness 15.69 µm vs 4.96 µm, $p < 0.0001$). This thickening depended on an accumulation of collagen

Accepted Article

deposit (Fig. 1C). The above results suggest that sunitinib increases the perivascular mesenchyme in ccRCC.

We investigated whether this increase in vascular wall thickness was linked to an increase in CAFs. To assess the contribution of CAFs to the vascular changes induced by sunitinib,

To assess the contribution of CAFs to vascular changes induced by sunitinib, we performed immunohistochemical examinations (Fig. 2A). CD31 staining validated the presence of blood vessels. The positivity for FAP and SMA on samples from patients treated with sunitinib, and their absence for patients without neoadjuvant sunitinib, support the hypothesis of an involvement of CAF in the observed vascular modifications.

We also analyzed the previously described CAF signature including FAP, SMA, COL1A1, TGFB1, LOXL2 and PLOD3 (8). Most of the mRNAs included in the CAFs signature were overexpressed in neoadjuvant as compared to control cases (Fig. 2B, FAP ($p=0.0424$), SMA ($p=0.0115$), COL1A1 ($p=0.0031$), TGFB1 ($p=0.0321$)). A trend was found for LOXL2 ($p=0.1290$) and PLOD3 ($p=0.0534$) mRNA. These results suggest that sunitinib induces capillary wall thickening in ccRCC by promoting recruitment of CAFs.

CAFs are correlated to a poor prognosis in ccRCC

We therefore hypothesized that CAFs modify tumor behavior and promote aggressiveness and influence the prognosis. To explore these possibilities, we correlated clinical data to FAP expression levels since it is the most relevant marker of CAFs. Moreover, the expression of all genes included in the CAF signature is correlated with the expression of FAP (Table S1A). High FAP mRNA levels were correlated with shorter DFS and OS in non-metastatic (M0) patients, the study cohort 2 (Fig. 3A, DFS, $p=0.027$ and Fig. 3B, OS, $p=0.044$) and the TCGA M0 cohort (Fig. 3C, DFS, $p=0.045$ and Fig. 3D, OS, $p=0.008$). In the TCGA metastatic (M1) cohort, high FAP mRNA levels were also correlated with shorter PFS and OS (Fig. 3E, PFS, $p=0.054$ and Fig. 3F, OS, $p=0.022$).

Accepted Article

By analyzing the TCGA database, we confirmed that low expression of different genes included in the CAF signature is associated, like FAP expression, with a longer overall survival (Table S1B).

In addition, we performed a “CAF signature” scoring. M0 patients with a score between 4 and 6 had a shorter DFS (Fig. S2A, p = 0.0012) and OS (Fig. S2B, p = 0.005) as compared to patients with a lower score. M1 patients with a score between 4 and 6 had a shorter PFS (Fig. S2C, trend) and OS (Fig. S2D, p = 0.035) as compared to patients with a lower score.

The level of FAP mRNA is also correlated with tumor stage (Fig. S1C, p=0.000793). These results show that the presence of CAFs is an adverse factor in the outcome of ccRCC.

CAFs are associated with lymphatic development and node dissemination

The perivascular topography of CAFs, their adverse impact on prognosis and the correlation between the presence of CAFs and metastasis suggested a relationship between CAFs and mechanisms of angio-lymphangiogenesis. The pivotal role of lymphatic vessels in metastatic dissemination encouraged us to explore the link between the presence of CAFs and lymphatic development and node dissemination by using a “lymphatic gene signature” (9).

In the neoadjuvant cohort (study cohort 1), tumors from patients treated with sunitinib in a neoadjuvant setting overexpressed genes corresponding to the lymphatic signature mRNA compared to tumors of ccRCC patients treated by surgery alone (Fig. 4A). Indeed, VEGR3 (p=0.009), NPR2 (p=0.046), VEGFC (p=0.032), c-MET (p=ns), HGF (p=0.0046), podoplanin (p=0.053) and Lyve1 (p=0.001) mRNA were highly expressed in tumors from sunitinib-treated patients.

We hypothesized that sunitinib-naive tumors were already infiltrated by CAFs. In addition, the correlation between CAFs and the lymphatic signature in the neoadjuvant cohort encouraged us to evaluate the lymphatic signature in untreated tumors of the TCGA. As anticipated, a high level of FAP was correlated with the lymphatic signature (Fig. 4B, C). Moreover, patients with lymph node metastases (N+) presented elevated FAP mRNA levels as compared to patients without lymph node metastases (N0, Fig.

Accepted Article

4D, p=0.011). Additionally, patients whose tumors had a high expression of FAP developed more lymph node metastases (Fig. 4E, p=0.015).

Patients with distant metastases (M1) presented a higher level of FAP mRNA as compared to patients without distant metastases (M0, Fig. 4D, p=0.046). In addition, patients whose tumors had a higher level of FAP mRNA developed more distant metastases (Fig. 4E, p=0.038). Hence, the CAFs-mediated adverse effects in ccRCC involve lymphatic development, node invasion and and metastatic dissemination.

CAFs induce migration of ccRCC cells and reduce the access of sunitinib to tumor cells

It is accepted that CAFs derived from the trans-differentiation of resident fibroblasts present in the tumor microenvironment (10). Therefore, the link between sunitinib, CAFs and tumor behavior was further investigated. For that purpose, primary fibroblasts (FHN) were rendered resistant to sunitinib (FHNR, Figure 5A). Sunitinib stimulated the expression of FAP, HGF and SMA mRNA in FHN (Fig. 5B to D). Moreover, FHNR presented elevated FAP, HGF and SMA mRNA levels as compared to control FHN. This basal level was further increased by sunitinib (Fig. 5B to D). These results suggest that a long-lasting exposure of FHNR to sunitinib stimulates their differentiation toward CAFs. These results were further supported by an in vivo experiment (Fig. S3). Mice bearing experimental ccRCC were treated with sunitinib or with placebo (Fig. S3A). FAP and SMA mRNA levels were upregulated in tumors from mice treated with sunitinib as compared to the placebo group (p=0.0489, Fig. S3B and C). These results support a model whereby sunitinib activates the differentiation of tumor resident fibroblasts to CAFs.

To further understand the impact of CAFs on ccRCC cell behavior, we focused on in vitro characteristics of cell aggressiveness. Chemotaxis assays showed that FHN promote ccRCC cell migration. This property was further enhanced by FHNR (Fig. 5E). The mechanisms mediating CAF-dependent decreased efficacy of sunitinib on ccRCC cells were then investigated. We previously demonstrated that sunitinib is trapped in lysosomes in ccRCC cells preventing the access of the drug to the kinase domain of tyrosine kinase receptors present in the cytoplasm (15). We analyzed the ability of

Accepted Article

sunitinib to cross the upper part of a Boyden chamber coated with FHN or FHNR and to accumulate in ccRCC cells present in the lower part of the chamber. An empty Boyden chamber was used as a control (full capacity of ccRCC cell to trap sunitinib).

The FHN barrier decreased the uptake of sunitinib by ccRCC cells and FHNR further decreased this process (Fig. 5F). These differences were stable over time. This “CAF-like” property that prevented the access of sunitinib to ccRCC cells improved tumor cell survival (Fig. 5H).

Next, we evaluated the impact of an inhibitor of TGFβ receptor (TGFBR) (CAF inhibitor, LY2109761) on the viability of FHNR and 786-O ccRCC cells. TGFR inhibitor decreased the viability of FHNR while it has no effect on ccRCC cells (Fig. 5G). TGFR inhibitor reverse the FHNR barrier decreasing the uptake of sunitinib by ccRCC, thus allowing the accessibility of sunitinib to ccRCC cells and their death (Fig. 5H).

Hence, these results strongly suggest that the presence of CAFs within blood vessels constitutes a barrier preventing the access of sunitinib to tumor cells and therefore an indirect mechanism of resistance.

DISCUSSION

Besides confirming an adverse prognostic effect of CAFs on ccRCC we showed that sunitinib promotes the appearance of CAFs but CAFs decrease the efficacy of sunitinib on tumor cells.

Targeted antiangiogenic therapy has brought great progress in the therapeutic management of metastatic ccRCC (11). The modification of vessels and vascular network structure and architecture is the expected effect of antiangiogenic treatments (12). VEGFR-TKI induce tumor shrinkage via necrosis due to a cytotoxic effect on tumor cells but also due to devascularization (13).

In this study, we demonstrated that antiangiogenic therapies (VEGFR-TKI, sunitinib) modify vessel structure and the cellular environment by increasing CAFs. Such modifications lead to limited efficacy of the antiangiogenic treatment.

Accepted Article

After a transient period of therapeutic efficacy lasting about 6 to 15 months, ccRCC acquires resistance to antiangiogenic targeted therapy (5). In some cases, resistance mechanisms involve genetic alterations allowing the tumor to grow and to maintain vascularization independently of the HIF-VEGF pathway. The activation of ATP-binding cassette efflux transporters and lysosomal sequestration contribute to resistance to TKIs (14,15). In mice models, resistance is reversed by reimplantation of resistant tumor xenografts in untreated mice (5). This reversibility of resistance argues for microenvironment changes as one major underlying mechanism.

The impact of acquired changes in the vascular and perivascular environment on resistance mechanisms has already been studied, but with conflicting results. Tumor neovascularization consists in the rapid establishment of immature, incomplete, tortuous, dilated neo-vessels with suboptimal interconnections. These vessels are lined by endothelial cells with imperfect morphology and functionality. Antiangiogenic drugs can normalize this network, which improves both the vascular distribution of treatments and tumor perfusion (16).

We showed that in ccRCC, CAFs are key players in resistance to VEGFR-TKI. This phenomenon involves the tumor microenvironment and more specifically VEGFR-TKI-induced trans-differentiation of resident fibroblasts to CAFs. Induction of tumor resistance by CAFs has been demonstrated in some tumor models, including lung carcinoma (17) and cholangiocarcinoma (18). We clearly showed that ccRCC behaves equivalently, notably through CAF-mediated reduction access of tumor cells to sunitinib.

CAFs, located in the stroma and in contact with tumor cells and other cellular actors, promote tumor development by several mechanisms. In ovarian carcinoma, stromal cells are one of the major sources of angiogenic growth factors (19) that control vascular maturation and permeability (20). In glioblastomas, CAFs secrete PDGF-C inducing the proliferation of pericytes covering the vessels, reducing their diameter and their permeability (21). In addition to the resistance to treatments, we showed that CAFs had an adverse prognostic effect and were correlated with the occurrence of metastases.

In ccRCCs, the spread of tumor cells depends mainly on blood vessels. Lymph node invasion and metastatic dissemination via lymphatic vessels are rare. However, it is an

Accepted Article

important mechanism to consider as it correlates with a poor prognosis. In esophageal squamous cell carcinoma (39) and breast cancer (40), CAF promote lymph node invasion. These elements prompted us to investigate the link between CAF and lymphatic dissemination in ccRCCs.

We observed that CAFs, increased by VEGR-TKI, were correlated with lymphatic vessel development and lymph node spread. This accords with our previous demonstration that VEGR-TKI stimulate the production of VEGFC by tumor cells resulting in the development of lymphatic vessels (22).

Our results agree with those of Peio Errarte *et al* in a series of 59 metastatic ccRCC (23,24). To explain this finding, we have shown that *in vitro* CAFs promote the migration of ccRCC. In a breast cancer model, CAFs induce microvascular disruption. This increase in vascular permeability stimulates the vascular transmigration of cancer cells (25).

The CAF-mediated epithelial-mesenchymal transition (EMT) of tumor cells may also explain their role in tumor aggressiveness. In a breast carcinoma model, CAFs and the extracellular matrix they deposit are aligned in a parallel pattern, inducing malignant epithelial cells to assume a mesenchymal morphology that was associated with increased dissemination and metastasis (26). In endometrial carcinomas, CAFs induce EMT through the secretion of cytokines, including TGF-β and HGF. This increases the invasion and migration of tumor cells and promotes metastasis (27). By analogy, a similar mechanism should occur in ccRCC. TGF-β is secreted by CAFs and by tumor cells and participates in the proliferation of both cell types (28,29). Through autocrine and paracrine mechanisms, the CAF-tumor cell interactions contribute to sarcomatoid transformation, cell migration and the appearance of metastases.

The presence of CAFs correlates with progression and poor prognosis in gastric cancer. The specific mechanism by which CAFs promote dissemination of gastric cancer involves β1 integrin, a membrane receptor controlling cell adhesion and metastatic dissemination of tumor cells. CAFs, via overexpression of Gal-1, participate in the upregulation of β1 integrin in gastric cancer and then facilitate gastric cancer cell migration and invasion (30).

Accepted Article

Prior to 2019, the first line treatment for ccRCC was VEGFR-TKI. Recently, immunotherapies targeting the PD1 and CTLA4 pathways have dramatically improved patient management. They are now standard treatment either alone or in combination with VEGF-TKI (31)(32). In this context, it is important to identify common mechanisms of resistance to these therapies. CAFs are involved in resistance to immunotherapies by limiting T cell infiltration. In colon carcinoma, lung carcinoma and melanoma models, CAFs constitutively express PD-L1 and negatively regulate tumor-associated T cell activation (33–35).

While immunotherapy may provide a long-lasting anti-tumor response, some patients are refractory. Mariathasan *et al* demonstrated that this lack of response was correlated with a TGF-β signature of metastatic urothelial carcinoma associated with a decrease in CD8+ T cells in the tumor areas (36). The infiltration of T cells in the tumor was restored by inhibiting TGF-β resulting in tumor regression.

In two separate studies conducted in mouse models of breast adenocarcinomas and pancreatic carcinomas, CAF-mediated resistance to immunotherapy was reversed (37,38). By targeting CXCL12 and TGF-β, CAF-dependent immune suppression was inhibited by promoting tumor T-cell infiltration. The anti-tumor response was synergized with immunotherapies targeting the PD-1 / PD-L1 axis.

We have explored one of the mechanisms involved in the resistance of ccRCC to VEGFR-TKI and described the involvement of CAFs in these mechanisms, as well as the impact of these cells on the prognosis of ccRCC.

Recently, “anti-CAF" immunotherapeutics or inhibitors gave promising results in several types of solid tumors. CAFs have been identified as one of the cellular actors interfering with T cell migration and activation, and CAF blockade is effective in restoring the response to immunotherapy. Thus, FAP-reactive CAR T cells have provided antitumor effect on models of lung and pancreatic cancer (41). It is also possible to counteract the pro-tumoral effects of CAFs by targeting downstream actors, for example TGFβ. This strategy has been successfully exploited using LY2109761, a TGFBR inhibitor in models of prostate cancers (42).

For the treatment of ccRCCs, immune checkpoint inhibitors (ICI) in combination with vascular endothelial growth factor receptor (VEGFR) tyrosine kinase (TKI) inhibitors is

Accepted Article

one of the most effective strategy. This combination is justified by the interaction between the immune and angiogenic systems. Angiogenic factors and their receptors can promote an immunosuppressive tumor microenvironment through a direct effect on immune cells. In addition, their role in antitumor immunity makes of CAFs promising therapeutic targets for the management of ccRCCs. These evidences favor the initiation of a clinical trial combining TKI, ICI and anti-CAF.

Conflict of Interest Statement: No conflicts exist

Acknowledgment

This work was supported by the Fondation de France, the Ligue Nationale contre le Cancer (Equipe Labellisée 2019), the French National Institute for Cancer Research (INCA), and the FX Mora and Cordon de vie Foundations. This study was conducted as part of the Centre Scientifique de Monaco Research Program, funded by the Government of the Principality of Monaco. The samples from Bordeaux and associated data were collected, selected and made available within the framework of the clinicobiological National Cancer Database Kidney UroCCR project supported by l'Institut National du Cancer (INCa). We thank the IRCAN core facilities (animal and cytometry facilities) for technical help. We thank also the Department of Pathology, especially Sandrine Destre and Marianne Goracci, for technical help.

FIGURE LEGENDS

Accepted Article

Figure 1. Sunitinib increases the thickness of the vessel wall.

Tumors from untreated ccRCC patients and tumors from patients treated with sunitinib in a neoadjuvant setting were compared. (**A**) Visualization of vessels by HES staining on tumor sections. Representative images are shown. (**B**) The thickness of the vessel wall was measured. (**C**) Detection of collagen by trichromatic staining on tumor sections. Representative images are shown. Statistical significance (p value) is indicated.

Figure 2. Sunitinib increases CAFs.

Tumors from untreated ccRCC patients and tumors from patients treated with sunitinib in a neoadjuvant setting were compared.

(**A**) Positive cytoplasmic staining for FAP (asterisk) and SMA in cells localized in the wall of a CD31 positive blood vessels, in tumors from sunitinib-treated patients. Negativity to FAP and CD31 staining was negative in tumors from untreated patients. (**B**) The levels of mRNA of the “CAF signature” were determined by qPCR. Statistical significance (p value) is indicated.

Figure 3. The amount of intra-tumor FAP mRNA correlated with an adverse outcome for ccRCC patients.

(**A and B**) Kaplan–Meier analysis of DFS (**A**) and OS (**B**) of M0 patients. DFS and OS were calculated from patient subgroups with FAP mRNA levels that were less or greater than the third quartile. Statistical significance (p value) is indicated. (**C to F**) ccRCC patients were analyzed for FAP mRNA levels. These results are based upon data generated by the TCGA Research Network and analyzed by cBioportal database. The levels of FAP mRNA in M0 ccRCC patients are correlated with DFS (**C**) or with OS (**D**). The levels of FAP mRNA in M1 ccRCC patients are correlated with PFS (**E**) or with OS (**F**). DFS / PFS / OS were calculated from patient subgroups with mRNA levels that were less or greater than the third quartile. Statistical significance (p value) is indicated.

Accepted Article

Figure 4. The amount of intra-tumor CAFs (FAP mRNA) correlated with lymphatic vessel development and lymph node metastasis.

(**A**) Tumors from untreated ccRCC patients and tumors from patients treated with sunitinib in a neoadjuvant setting were compared. The levels of mRNA of the "lymphatic signature" were determined by qPCR. Statistical significance (p value) is indicated. (**B to E**) These results are based upon data generated by the TCGA Research Network and analyzed by cBioportal database. (**B**) The levels of mRNA of the "lymphatic signature" (z-score) in ccRCC patients with FAP low were compared to the levels in ccRCC patients with FAP high. (**C**) Heatmaps for the relative expression of genes in 40 patients with low FAP expression and 40 patients with high FAP expression. (**D**) FAP mRNA (z-score) expression in i) non-lymph node metastasis (N0) and lymph node metastasis (N+) patients and in ii) non-metastatic (M0) and metastatic (M1) patients. (**E**) Lymph node metastasis (N+) and distant metastases (M1) in patients with low or high levels of FAP mRNA.

Figure 5. Sunitinib induces CAFs *in vitro*.

(A) FHN resistant to sunitinib (FHNR) were generated. FHN and FHNR were treated with 5µM sunitinib (suni) for 48h. Cell viability was measured by XTT assays. **(B to D)** FHN and FHNR were treated with 5µM sunitinib (suni) for 48h. The levels of FAP **(B)**, HGF **(C)** and SMA **(D)** mRNA were determined by qPCR. **(E)** 786 cells were seeded on the upper side of the filters and Boyden chambers were placed on 24-well plates containing FHN or FHNR at confluence and without serum. **(F)** FHN or FHNR were grown to confluency in a co-culture chamber. The empty chambers (0) or chambers containing FHN or FHNR were placed in contact with the 786-O cells. 5µM sunitinib was added in the upper chamber for different lengths of time (2 to 8h). The percentage of sunitinib having crossed and reached the 786-O cells was measured by cytometry. **(G)** 786-O (786) and FHNR cells were treated with 20µM LY2109761 (TGFR inhibitor) for 48h. Cell viability was measured by XTT assays. **(H)** FHN or FHNR were grown to confluency in a co-culture chamber. The empty chambers (0) or the chambers

Accepted Article

containing FHN or FHNR were placed in contact with 786-O cells. 5µM sunitinib with or without 20µM LY2109761 was added in the upper chamber for 8h. 48h afterwards, cell viability was measured by XTT assays. Results are presented as the mean of three independent experiments ± SEM. * $p<0.05$, ** $p<0.01$, *** $p<0.001$.

TABLE LEGENDS

Table 1

Characteristics of the patients included in the study (see Fig. 1 and 2).

Table 2

Characteristics of the patients included in the study (see Fig. 3).

REFERENCES

1. Palumbo C, Pecoraro A, Knipper S, Rosiello G, Luzzago S, Deuker M, et al. Contemporary Age-adjusted Incidence and Mortality Rates of Renal Cell Carcinoma: Analysis According to Gender, Race, Stage, Grade, and Histology. Eur Urol Focus. 23 mai 2020;

2. Moch H, Cubilla AL, Humphrey PA, Reuter VE, Ulbright TM. The 2016 WHO Classification of Tumours of the Urinary System and Male Genital Organs-Part A: Renal, Penile, and Testicular Tumours. Eur Urol. 2016;70(1):93‑105.

3. Ljungberg B, Albiges L, Abu-Ghanem Y, Bensalah K, Dabestani S, Fernández-Pello S, et al. European Association of Urology Guidelines on Renal Cell Carcinoma: The 2019 Update. Eur Urol. 2019;75(5):799‑810.

4. Atkins MB, Tannir NM. Current and emerging therapies for first-line treatment of metastatic clear cell renal cell carcinoma. Cancer Treat Rev. nov 2018;70:127‑37.

5. Rini BI, Atkins MB. Resistance to targeted therapy in renal-cell carcinoma. Lancet Oncol. oct 2009;10(10):992‑1000.

6. Mier JW. The tumor microenvironment in renal cell cancer. Curr Opin Oncol.

Accepted Article

2019;31(3):194‑9.

7. Kuzet S-E, Gaggioli C. Fibroblast activation in cancer: when seed fertilizes soil. Cell Tissue Res. 2016;365(3):607‑19.

8. Hanley CJ, Noble F, Ward M, Bullock M, Drifka C, Mellone M, et al. A subset of myofibroblastic cancer-associated fibroblasts regulate collagen fiber elongation, which is prognostic in multiple cancers. Oncotarget. 2 févr 2016;7(5):6159‑74.

9. Podgrabinska S, Braun P, Velasco P, Kloos B, Pepper MS, Skobe M. Molecular characterization of lymphatic endothelial cells. Proc Natl Acad Sci USA. 10 déc 2002;99(25):16069‑74.

10. Kojima Y, Acar A, Eaton EN, Mellody KT, Scheel C, Ben-Porath I, et al. Autocrine TGF-beta and stromal cell-derived factor-1 (SDF-1) signaling drives the evolution of tumor-promoting mammary stromal myofibroblasts. Proc Natl Acad Sci USA. 16 nov 2010;107(46):20009‑14.

11. Motzer RJ, Hutson TE, Tomczak P, Michaelson MD, Bukowski RM, Rixe O, et al. Sunitinib versus interferon alfa in metastatic renal-cell carcinoma. N Engl J Med. 11 janv 2007;356(2):115‑24.

12. Kim E, Moore J, Huang J, Soffer S, Manley CA, O'Toole K, et al. All angiogenesis is not the same: Distinct patterns of response to antiangiogenic therapy in experimental neuroblastoma and Wilms tumor. J Pediatr Surg. févr 2001;36(2):287‑90.

13. Sirous R, Henegan JC, Zhang X, Howard CM, Souza F, Smith AD. Metastatic renal cell carcinoma imaging evaluation in the era of anti-angiogenic therapies. Abdom Radiol (NY). 2016;41(6):1086‑99.

14. Makhov P, Joshi S, Ghatalia P, Kutikov A, Uzzo RG, Kolenko VM. Resistance to Systemic Therapies in Clear Cell Renal Cell Carcinoma: Mechanisms and Management Strategies. Mol Cancer Ther. 2018;17(7):1355‑64.

15. Giuliano S, Cormerais Y, Dufies M, Grépin R, Colosetti P, Belaid A, et al. Resistance to sunitinib in renal clear cell carcinoma results from sequestration in lysosomes and inhibition of the autophagic flux. Autophagy. 2015;11(10):1891‑904.

16. Jain RK. Normalization of tumor vasculature: an emerging concept in antiangiogenic therapy. Science. 7 janv 2005;307(5706):58‑62.

17. Wang W, Li Q, Yamada T, Matsumoto K, Matsumoto I, Oda M, et al. Crosstalk to

Accepted Article

stromal fibroblasts induces resistance of lung cancer to epidermal growth factor receptor tyrosine kinase inhibitors. Clin Cancer Res. 1 nov 2009;15(21):6630‑8.

18. Vaquero J, Lobe C, Tahraoui S, Clapéron A, Mergey M, Merabtene F, et al. The IGF2/IR/IGF1R Pathway in Tumor Cells and Myofibroblasts Mediates Resistance to EGFR Inhibition in Cholangiocarcinoma. Clin Cancer Res. 01 2018;24(17):4282‑96.

19. Thijssen VLJL, Brandwijk RJMGE, Dings RPM, Griffioen AW. Angiogenesis gene expression profiling in xenograft models to study cellular interactions. Exp Cell Res. 1 oct 2004;299(2):286‑93.

20. Gilad AA, Israely T, Dafni H, Meir G, Cohen B, Neeman M. Functional and molecular mapping of uncoupling between vascular permeability and loss of vascular maturation in ovarian carcinoma xenografts: the role of stroma cells in tumor angiogenesis. Int J Cancer. 1 nov 2005;117(2):202‑11.

21. di Tomaso E, London N, Fuja D, Logie J, Tyrrell JA, Kamoun W, et al. PDGF-C induces maturation of blood vessels in a model of glioblastoma and attenuates the response to anti-VEGF treatment. PLoS ONE. 2009;4(4):e5123.

22. Dufies M, Giuliano S, Ambrosetti D, Claren A, Ndiaye PD, Mastri M, et al. Sunitinib Stimulates Expression of VEGFC by Tumor Cells and Promotes Lymphangiogenesis in Clear Cell Renal Cell Carcinomas. Cancer Res. 01 2017;77(5):1212‑26.

23. Errarte P, Guarch R, Pulido R, Blanco L, Nunes-Xavier CE, Beitia M, et al. The Expression of Fibroblast Activation Protein in Clear Cell Renal Cell Carcinomas Is Associated with Synchronous Lymph Node Metastases. PLoS ONE. 2016;11(12):e0169105.

24. López JI, Errarte P, Erramuzpe A, Guarch R, Cortés JM, Angulo JC, et al. Fibroblast activation protein predicts prognosis in clear cell renal cell carcinoma. Hum Pathol. 2016;54:100‑5.

25. Choi YP, Lee JH, Gao M-Q, Kim BG, Kang S, Kim SH, et al. Cancer-associated fibroblast promote transmigration through endothelial brain cells in three-dimensional in vitro models. Int J Cancer. 1 nov 2014;135(9):2024‑33.

26. Dumont N, Liu B, Defilippis RA, Chang H, Rabban JT, Karnezis AN, et al. Breast fibroblasts modulate early dissemination, tumorigenesis, and metastasis through

Accepted Article

alteration of extracellular matrix characteristics. Neoplasia. mars 2013;15(3):249‑62.

27. Wang X, Zhang W, Sun X, Lin Y, Chen W. Cancer-associated fibroblasts induce epithelial-mesenchymal transition through secreted cytokines in endometrial cancer cells. Oncol Lett. avr 2018;15(4):5694‑702.

28. Tretbar S, Krausbeck P, Müller A, Friedrich M, Vaxevanis C, Bukur J, et al. TGF-β inducible epithelial-to-mesenchymal transition in renal cell carcinoma. Oncotarget. 19 févr 2019;10(15):1507‑24.

29. Ananth S, Knebelmann B, Grüning W, Dhanabal M, Walz G, Stillman IE, et al. Transforming growth factor beta1 is a target for the von Hippel-Lindau tumor suppressor and a critical growth factor for clear cell renal carcinoma. Cancer Res. 1 mai 1999;59(9):2210‑6.

30. He X-J, Tao H-Q, Hu Z-M, Ma Y-Y, Xu J, Wang H-J, et al. Expression of galectin-1 in carcinoma-associated fibroblasts promotes gastric cancer cell invasion through upregulation of integrin β1. Cancer Sci. nov 2014;105(11):1402‑10.

31. Motzer RJ, Tannir NM, McDermott DF, Arén Frontera O, Melichar B, Choueiri TK, et al. Nivolumab plus Ipilimumab versus Sunitinib in Advanced Renal-Cell Carcinoma. N Engl J Med. 5 avr 2018;378(14):1277‑90.

32. Rini BI, Plimack ER, Stus V, Gafanov R, Hawkins R, Nosov D, et al. Pembrolizumab plus Axitinib versus Sunitinib for Advanced Renal-Cell Carcinoma. N Engl J Med. 21 mars 2019;380(12):1116‑27.

33. Pinchuk IV, Saada JI, Beswick EJ, Boya G, Qiu SM, Mifflin RC, et al. PD-1 ligand expression by human colonic myofibroblasts/fibroblasts regulates CD4+ T-cell activity. Gastroenterology. oct 2008;135(4):1228‑37, 1237.e1-2.

34. Nazareth MR, Broderick L, Simpson-Abelson MR, Kelleher RJ, Yokota SJ, Bankert RB. Characterization of human lung tumor-associated fibroblasts and their ability to modulate the activation of tumor-associated T cells. J Immunol. 1 mai 2007;178(9):5552‑62.

35. Khalili JS, Liu S, Rodríguez-Cruz TG, Whittington M, Wardell S, Liu C, et al. Oncogenic BRAF(V600E) promotes stromal cell-mediated immunosuppression via induction of interleukin-1 in melanoma. Clin Cancer Res. 1 oct 2012;18(19):5329‑40.

36. Mariathasan S, Turley SJ, Nickles D, Castiglioni A, Yuen K, Wang Y, et al. TGFβ

Accepted Article

attenuates tumour response to PD-L1 blockade by contributing to exclusion of T cells. Nature. 22 2018;554(7693):544‑8.

37. Feig C, Jones JO, Kraman M, Wells RJB, Deonarine A, Chan DS, et al. Targeting CXCL12 from FAP-expressing carcinoma-associated fibroblasts synergizes with anti-PD-L1 immunotherapy in pancreatic cancer. Proc Natl Acad Sci USA. 10 déc 2013;110(50):20212‑7.

38. Holmgaard RB, Schaer DA, Li Y, Castaneda SP, Murphy MY, Xu X, et al. Targeting the TGFβ pathway with galunisertib, a TGFβRI small molecule inhibitor, promotes anti-tumor immunity leading to durable, complete responses, as monotherapy and in combination with checkpoint blockade. J Immunother Cancer. 04 2018;6(1):47.

39. Kashima H, Noma K, Ohara T, Kato T, Katsura Y, Komoto S, et al. Cancer-associated fibroblasts (CAFs) promote the lymph node metastasis of esophageal squamous cell carcinoma. Int J Cancer. 15 févr 2019;144(4):828‑40.

40. Pelon F, Bourachot B, Kieffer Y, Magagna I, Mermet-Meillon F, Bonnet I, et al. Cancer-associated fibroblast heterogeneity in axillary lymph nodes drives metastases in breast cancer through complementary mechanisms. Nat Commun. 21 janv 2020;11(1):404.

41. Lo A, Wang L-CS, Scholler J, Monslow J, Avery D, Newick K, et al. Tumor-Promoting Desmoplasia Is Disrupted by Depleting FAP-Expressing Stromal Cells. Cancer Res. 15 juill 2015;75(14):2800‑10.

42. Sun D-Y, Wu J-Q, He Z-H, He M-F, Sun H-B. Cancer-associated fibroblast regulate proliferation and migration of prostate cancer cells through TGF-β signaling pathway. Life Sci. 15 oct 2019;235:116791.

Accepted Article

GROUP	**CT**	**Sunitinib neoadjuvant**
Number of patients	11	11
Sex - Woman - Man	2 (18%) 9 (82%)	2 (18%) 9 (82%)
AT DIAGNOSIS		
Age	57 (42-86)	55 (32-79)
Furhman grade - 3 - 4	8 (73%) 3 (27%)	8 (73%) 3 (27%)
Metastatic status pM - M0 - M1	2 (18%) 9 (82%)	2 (18%) 9 (82%)
Lymph node status pN - N0 - N1	8 (73%) 3 (27%)	7 (64%) 4 (36%)
Number of metastasis - 0 - 1 - 2	2 (18%) 5 (46%) 4 (36%)	2 (18%) 4 (36%) 5 (46%)
TREATMENT (NEOADJUVANT)		
Duration of treatment (months)	NA	4.5 (2-9)

TABLE 1

Accepted Article

GROUP	
Number of patients	38
Sex - Woman - Man	14 (36.8%) 24 (63.2%)
Age	62 (42-82)
Furhman grade - 2 - 3 - 4	17 (44.7%) 16 (42.1%) 5 (13.2%)
pM status - M0	38 (100%)
pN status - N0 - N1	34 (89.5%) 4 (10.5%)
pT status - 1 - 2 - 3	17 (44.7%) 6 (15.8%) 15 (39.5%)

TABLE 2

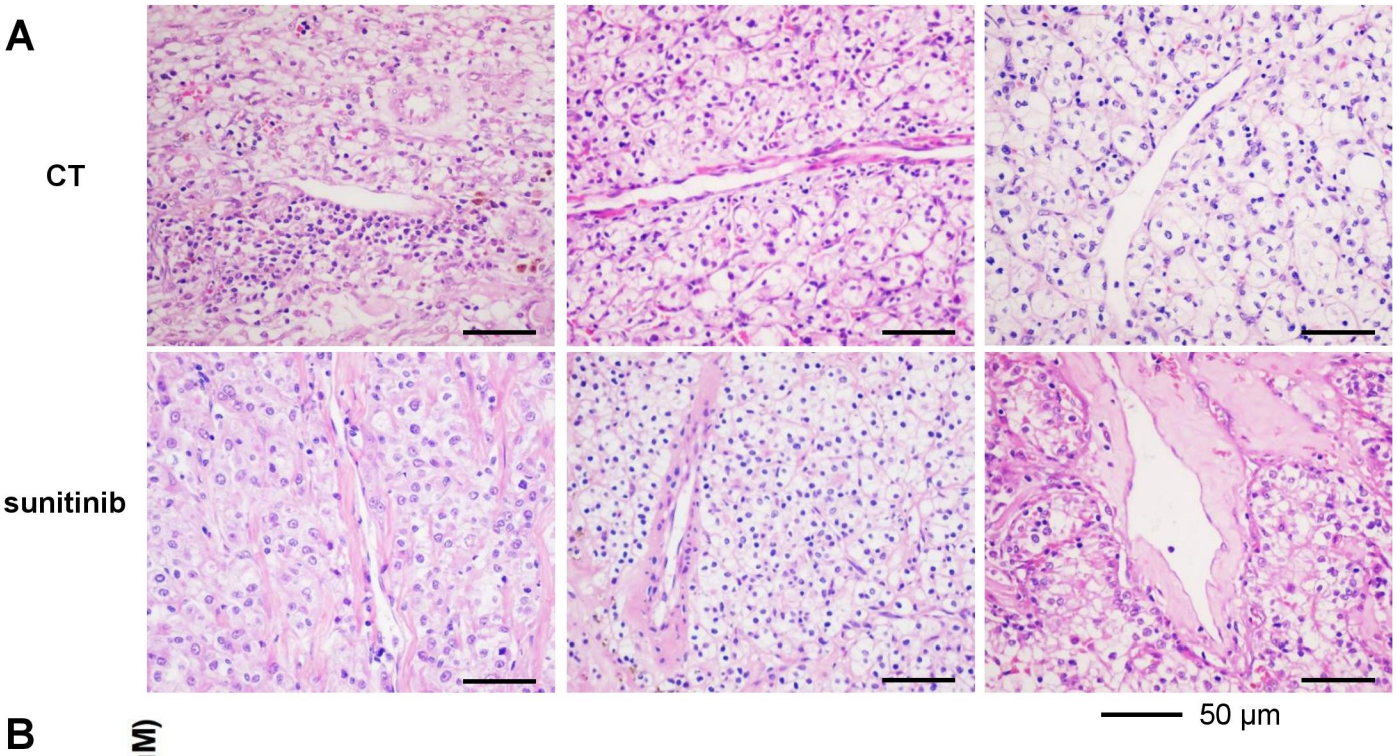

B

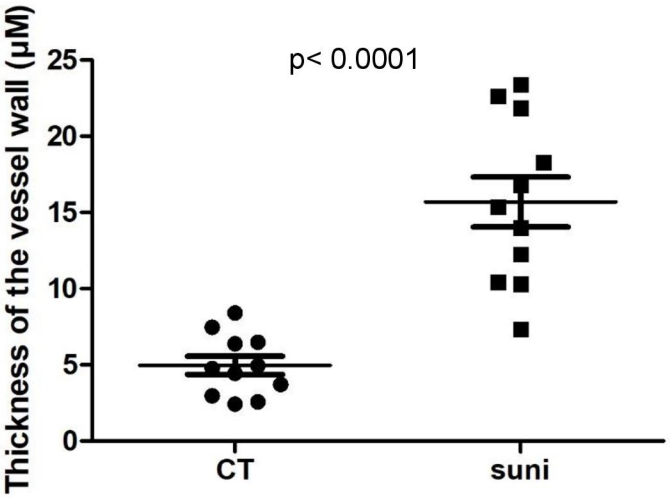

	Thickness median (µM)
CT	4.96 ± 0.60
sunitinib	15.69 ± 1.63

C

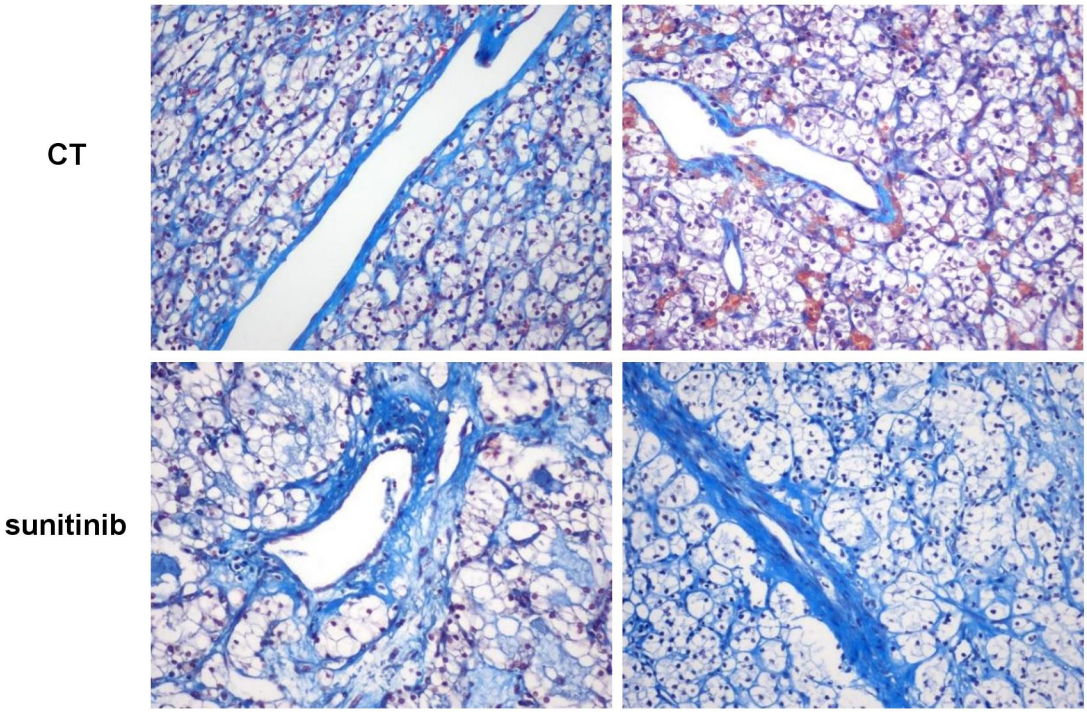

Figure 1

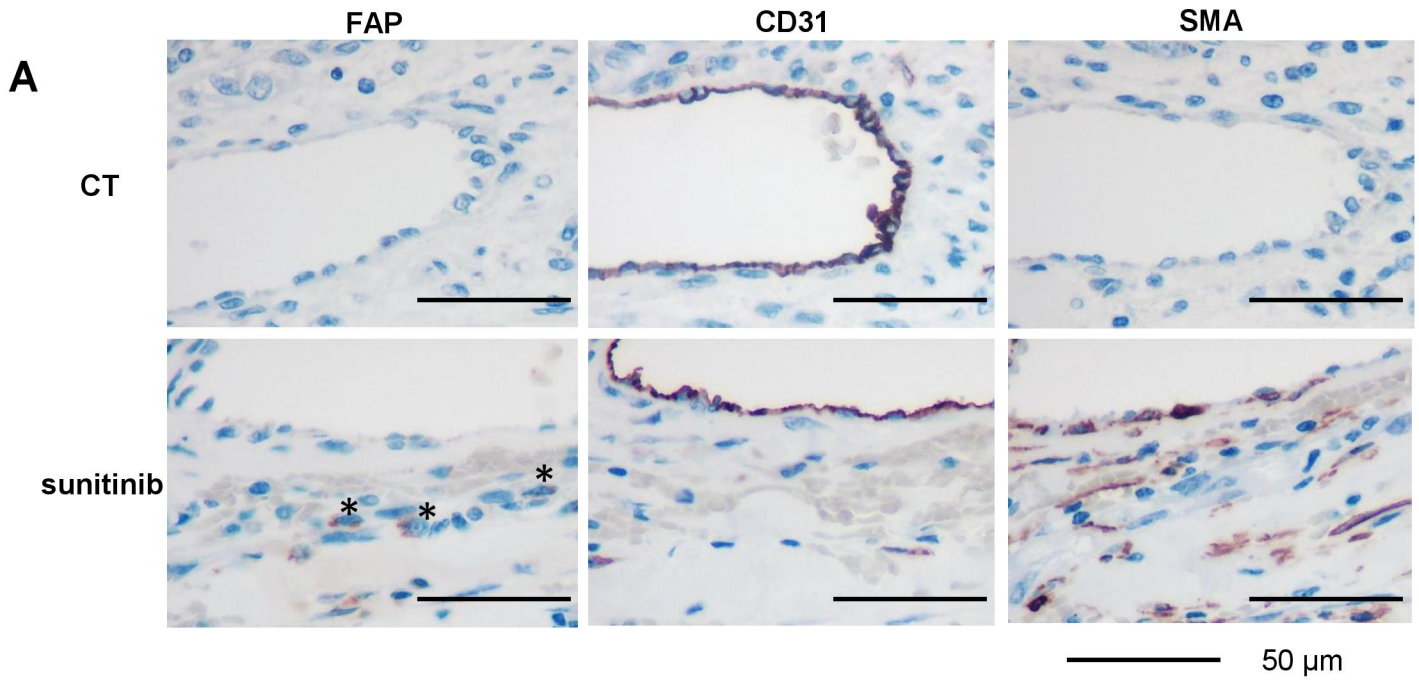
A
FAP
CD31
SMA
CT
sunitinib
50 µm

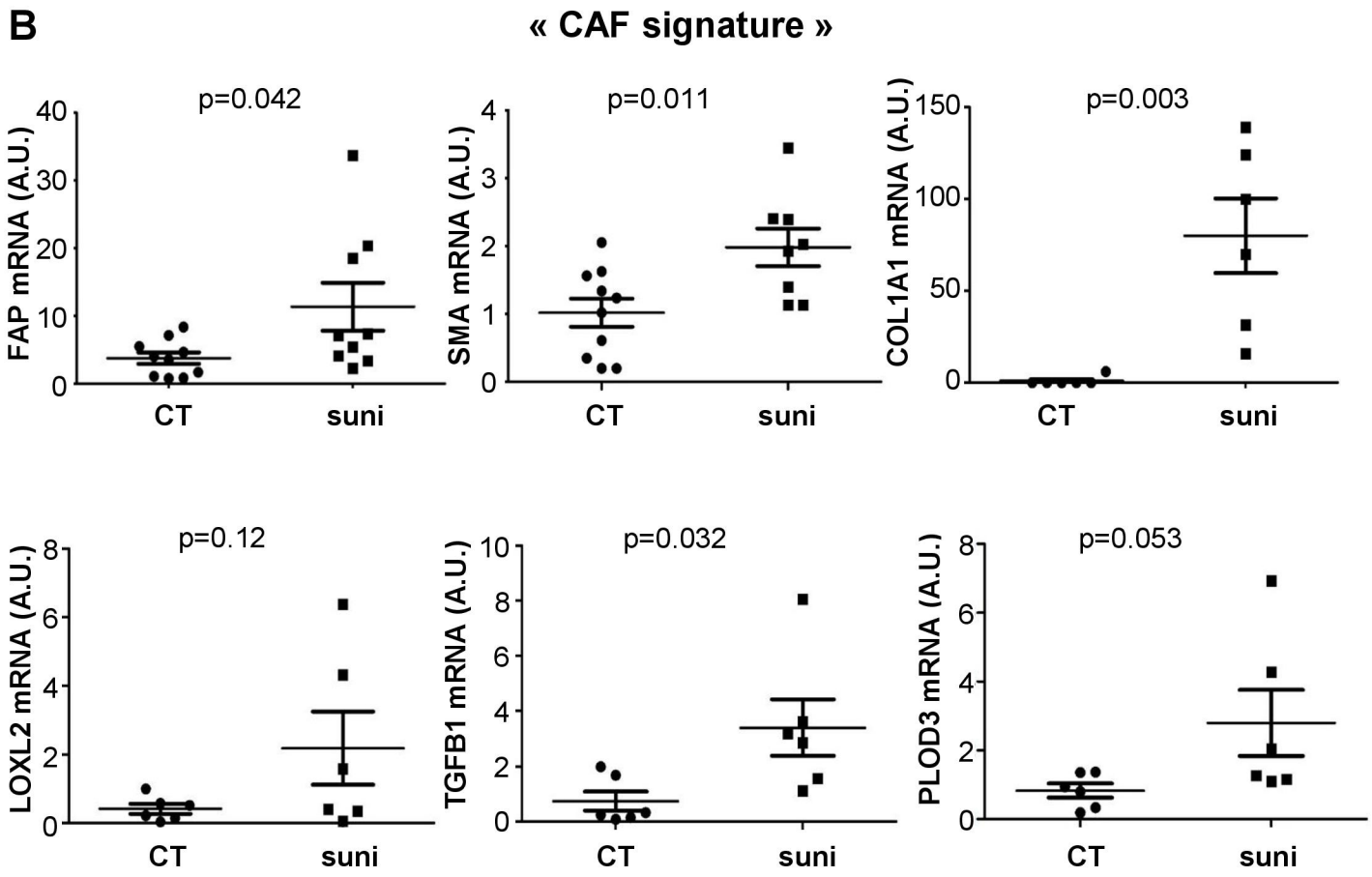
B
« CAF signature »
FAP mRNA (A.U.)
p=0.042
SMA mRNA (A.U.)
p=0.011
COL1A1 mRNA (A.U.)
p=0.003
LOXL2 mRNA (A.U.)
p=0.12
TGFB1 mRNA (A.U.)
p=0.032
PLOD3 mRNA (A.U.)
p=0.053
CT
suni

Figure 2

Study cohort 2 – M0

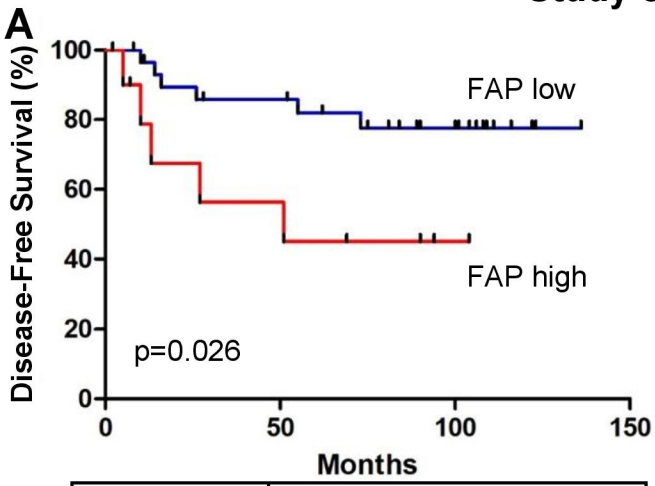

	Median survival (Months)
Low FAP	Undefined
High FAP	51

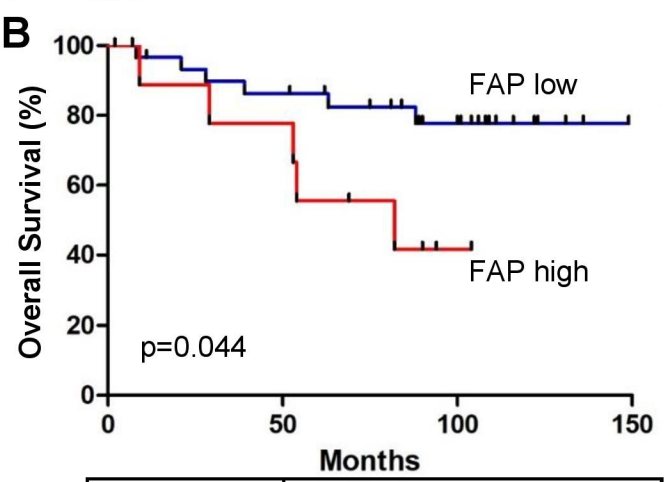

	Median survival (Months)
Low FAP	Undefined
High FAP	82

TCGA cohort – M0

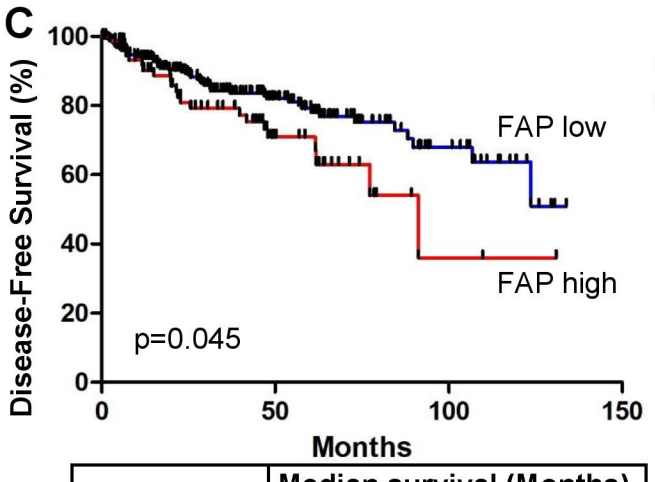

	Median survival (Months)
Low FAP	Undefined
High FAP	91.33

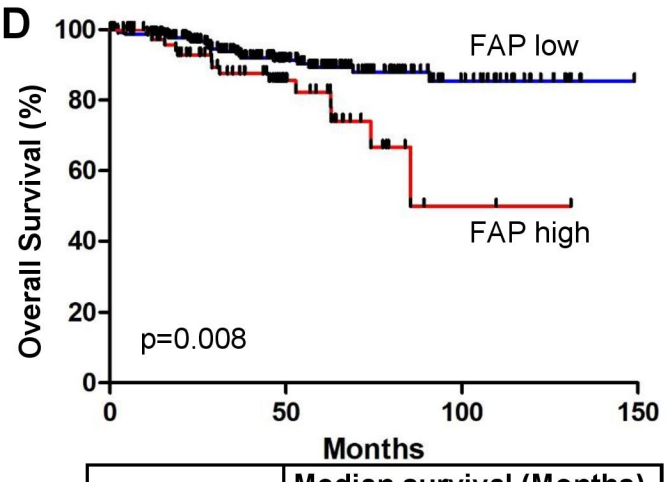

	Median survival (Months)
Low FAP	Undefined
High FAP	85.45

TCGA cohort – M1

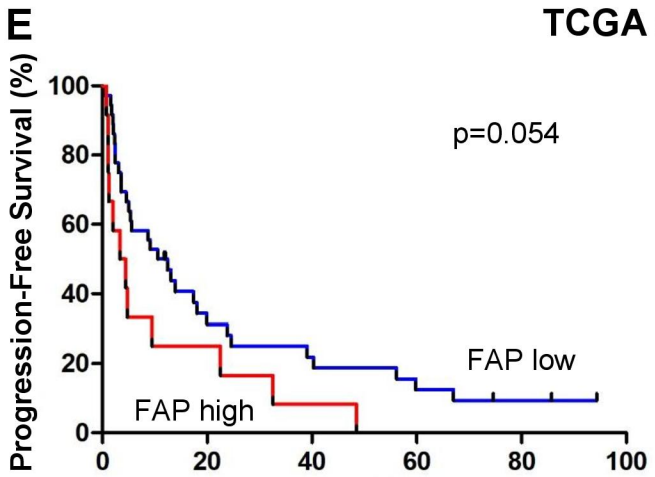

	Median survival (Months)
Low FAP	11.49
High FAP	3.94

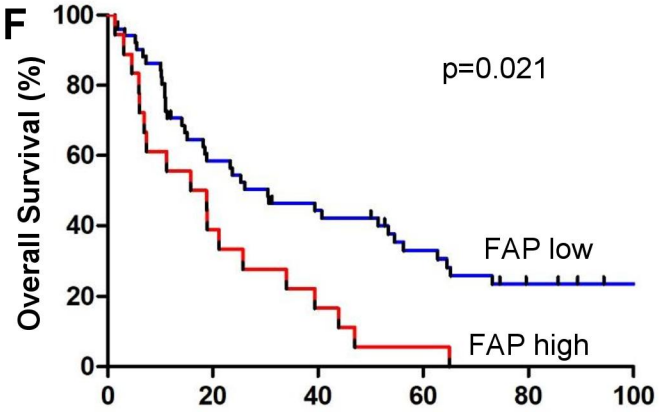

	Median survival (Months)
Low FAP	30.45
High FAP	17.28

Figure 3

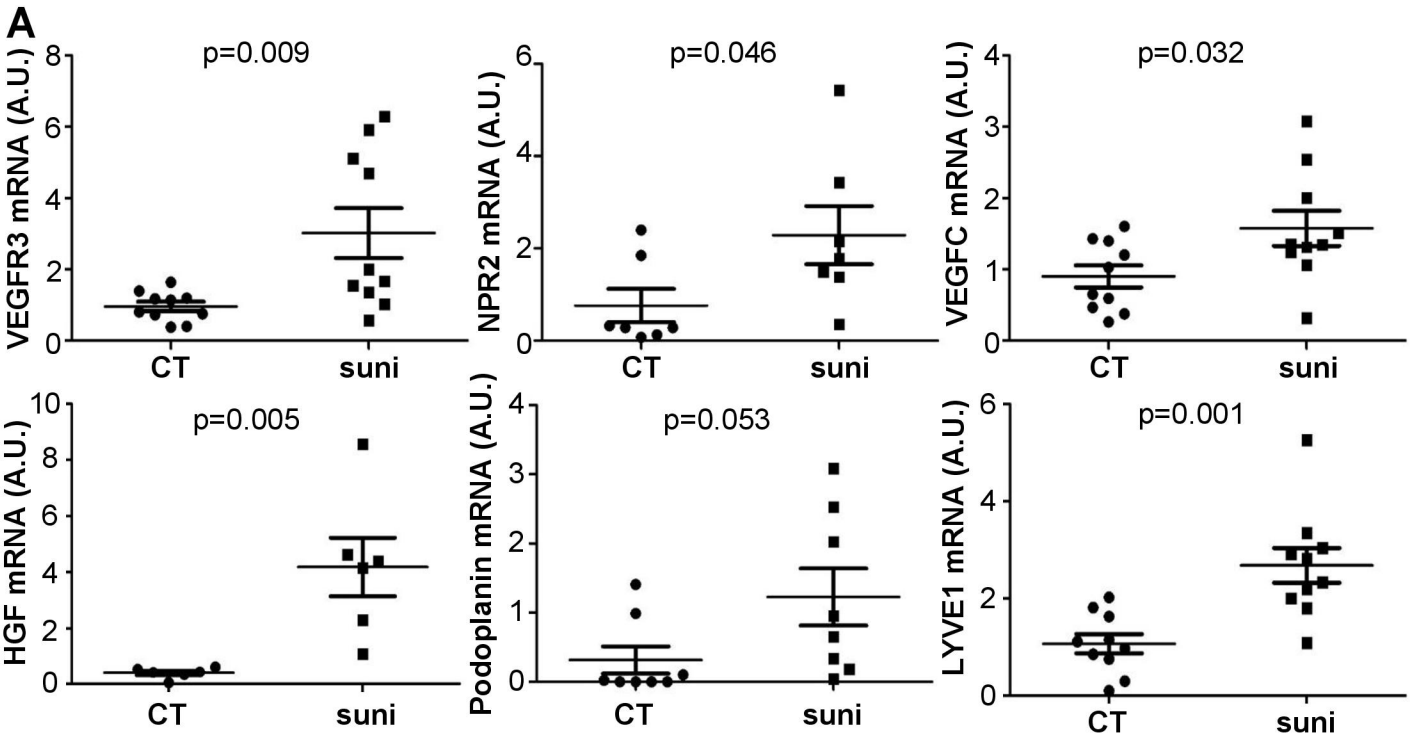

B

Gene (z-score)	FAP low	FAP high	p value
HGF	-0.019	0.773	< 0.0001
NRP2	-0.16	0.53	< 0.0001
VEGFC	-0.178	0.419	< 0.0001
VEGFR3	-0.122	0.153	0.0046
Podoplanin	-0.087	0.17	< 0.0001
LYVE1	-0.19	0.324	< 0.0001

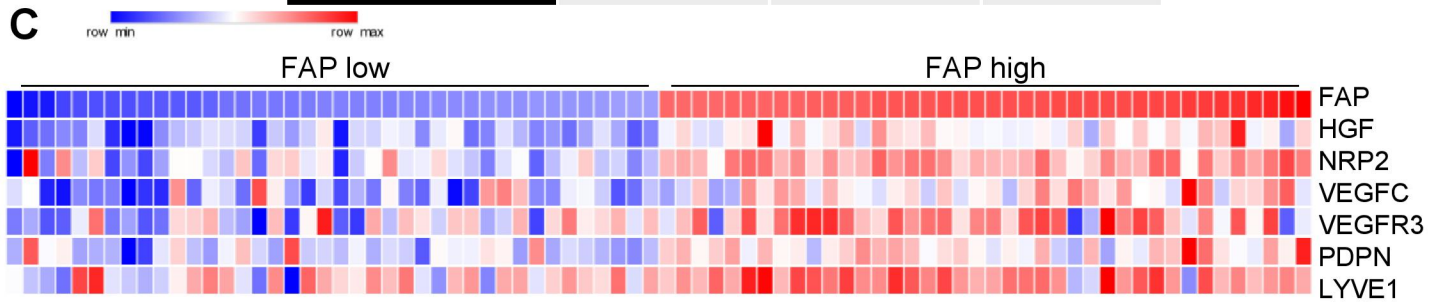

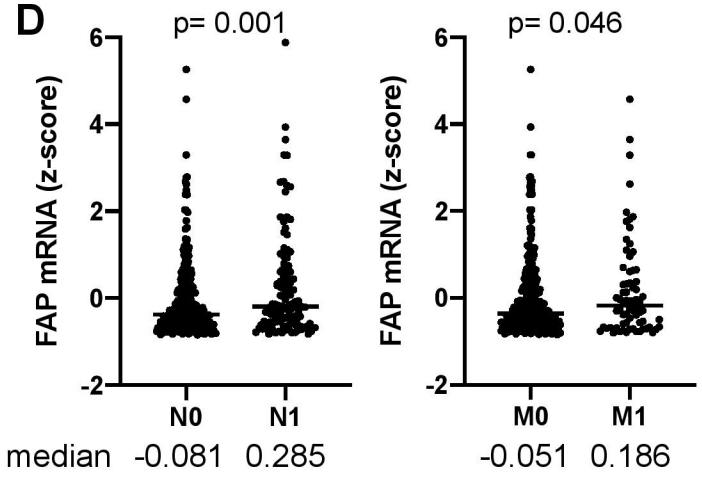

E

p=0.015	FAP low	FAP high
N0	252 (76,8%)	73 (65,2%)
N+	76 (23,2%)	39 (34,8%)

p=0.038	FAP low	FAP high
M0	286 (86.4%)	90 (78,2%)
M1	45 (13.6%)	25 (21.7%)

Figure 4

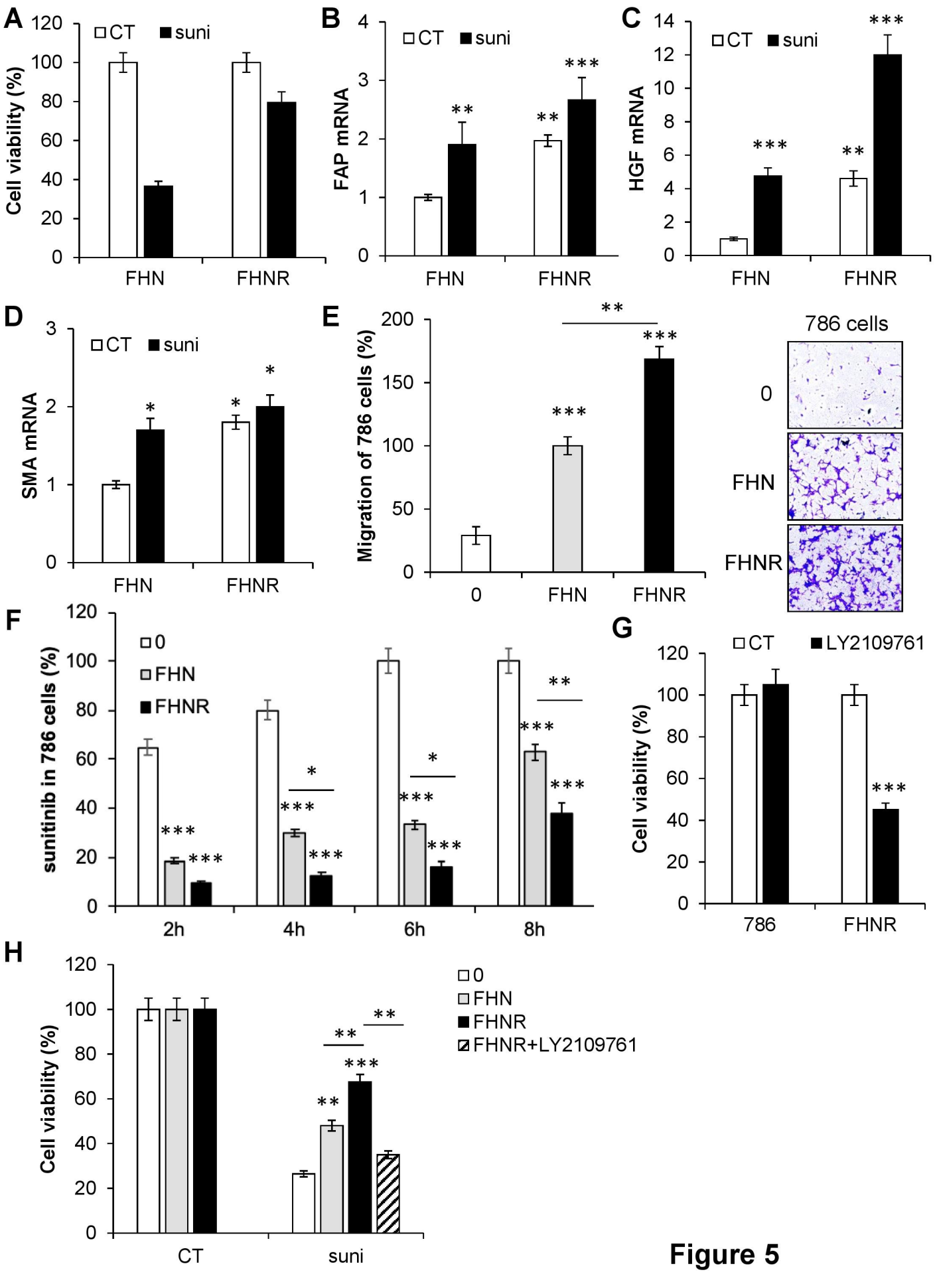
A
Cell viability (%)
CT
suni
FHN
FHNR
B
FAP mRNA
C
HGF mRNA
D
SMA mRNA
E
Migration of 786 cells (%)
786 cells
0
F
sunitinib in 786 cells (%)
2h
4h
6h
8h
G
LY2109761
786
H
FHNR+LY2109761

Figure 5